



# Soil Fungal Community Structure and Function Shift during a Disease-Driven Forest Succession

Zhao-lei Qu,<sup>a</sup> Ahmed Braima,<sup>a</sup> Bing Liu,<sup>a,b</sup> Yang Ma,<sup>a</sup>  Hui Sun<sup>a</sup>

<sup>a</sup>Collaborative Innovation Center of Sustainable Forestry in Southern China, College of Forestry, Nanjing Forestry University, Nanjing, China

<sup>b</sup>Yangzhou Polytechnic College, Yangzhou, China

Zhao-lei Qu and Ahmed Braima contributed equally to the work. Author order was determined in order of increasing seniority.

**ABSTRACT** Forest succession is important for sustainable forest management in terrestrial ecosystems. However, knowledge about the response of soil microbes to forest disease-driven succession is limited. In this study, we investigated the soil fungal biomass, soil enzyme activity, and fungal community structure and function in forests suffering succession processes produced by pine wilt disease from conifer to broadleaved forests using Illumina Miseq sequencing coupled with FUNGuild analysis. The results showed that the broadleaved forest had the highest fungal biomass and soil enzyme activities in C, N, and S cycles, whereas the conifer forest had the highest enzyme activity in the P cycle. Along the succession, the fungal diversity and richness significantly increased ( $P < 0.05$ ). The fungal communities were dominated by Ascomycota (42.0%), Basidiomycota (38.0%), and Mortierellomycota (9.5%), among which the abundance of Ascomycota significantly increased ( $P < 0.05$ ), whereas that of Basidiomycota and Mortierellomycota decreased ( $P < 0.05$ ). The abundance of species *Mortierella humilis*, *Lactarius salmonicolor*, and *Russula sanguinea* decreased, whereas that of *Mortierella minutissima* increased ( $P < 0.05$ ). The forests in different succession stages formed distinct fungal communities and functional structures ( $P < 0.05$ ). Functionally, the saprotrophs, symbiotrophs, and pathotrophs were the dominant groups in the conifer, mixed, and broadleaved forests, respectively. Soil pH and soil organic carbon were the key factors influencing the fungal community and functional structures during the succession. These findings provide useful information for better understanding the plant-microbe interaction during forest succession caused by forest disease.

**IMPORTANCE** The studies on soil fungal communities in disease-driven forest succession are rare. This study showed that during the disease-driven forest succession, the soil enzyme activity, soil fungal diversity, and biomass increased along succession. The disease-driven forest succession changed the soil fungal community structure and function, in which the symbiotrophs were the most dominant group along the succession. These findings provide useful information for better understanding the plant-microbe interaction during forest succession caused by forest disease.

**KEYWORDS** fungal community, forest succession, enzyme activity, pine wilt disease, microbe-plant interactions

Forest succession caused by natural disturbance can affect a wide array of terrestrial ecosystem processes and is important for sustainable forest management (1). The ecological linkages between aboveground and belowground biota during forest succession have been considered an important mechanism in forest development and succession (2). For example, wildfire disturbance can change the forest soil chemistry and soil enzyme activity, which reduces the diversity and abundance of mycorrhizal fungi (3). The plant changes caused by succession can affect the soil microbial community, which, in turn, can regulate the plant growth via moderating the decomposition of soil organic matter (SOM)

**Editor** Junhyun Jeon, Yeungnam University

**Copyright** © 2022 Qu et al. This is an open-access article distributed under the terms of the [Creative Commons Attribution 4.0 International license](https://creativecommons.org/licenses/by/4.0/).

Address correspondence to Hui Sun, [hui.sun@njfu.edu.cn](mailto:hui.sun@njfu.edu.cn).

The authors declare no conflict of interest.

**Received** 4 March 2022

**Accepted** 5 August 2022

**Published** 8 September 2022

(4). Many studies have focused on the effects of forest succession on the aboveground plant community assembly (5), tree architecture variability (6), and plant nutrient use strategies (7), but knowledge on the dynamics of soil microbial communities and their functions during the disease-driven forest succession process is limited.

Soil microbes generally have rapid responses and high turnover rates in response to environmental disturbance, which could provide additional information on the forest succession mechanism; for example, plant species can strongly affect the soil microbial community structure and functions through the allocation of plant carbon and other nutrients (8, 9). Soil abiotic properties, including pH and nutrient availability, are key regulators that link plant performance with soil microbial communities (10, 11). Soil fungi represent an essential functional component of soil as decomposers, symbionts, and pathogens, in which saprophytic soil fungi can decompose soil substrates and increase the soil nutrient cycle, while ectomycorrhizal fungi, such as symbiotrophs, are known to enhance the nutritional condition of plants (12, 13). Fungal biomass and microbial enzyme activity are sensitive to changes in soil characteristics (14). In general, the deciduous forest has significantly higher soil fungal biomass when compared with that of the conifer forest (15). The extracellular soil enzymes produced by fungi can be involved in soil carbon (C), nitrogen (N), and phosphorus (P) cycles, which have a significant effect on the initial decomposition of plant litter (16, 17). Many environmental factors, such as plant species, can influence soil enzyme activities (18, 19). Therefore, soil enzyme activities and the fungal biomass are often used as indicators to reflect changes in the ecosystem due to their rapid response to environmental changes.

Forest decline has contributed to changes in soil nutrients and properties. The most recent outbreak caused by mountain pine beetle (*Dendroctonus ponderosae*) has affected more than 14 million hectares of forest land and triggered forest decline in western Canada (20). Compared with undisturbed stands, beetle-killed lodgepole pine (*Pinus contorta* var. *latifolia* Engelm.) stands have caused a decrease in soil phenolic content and increased soil moisture content and available nutrients (21, 22). Increased soil phenolics have led to decreased colonization rates in ectomycorrhizal fungi (23). Soil phenolics belong to a class of carbon-rich plant secondary compounds and are known to affect nutrient availability, especially nitrogen (23, 24). A previous study has demonstrated a decreased richness of ectomycorrhizal fungi in beetle-killed pine stands (25). However, there is a lack of research on the response of soil microbes to forest decline induced by forest disease.

Pine wilt disease (PWD) caused by pinewood nematode (PWN) *Bursaphelenchus xylophilus* is one of the most serious diseases worldwide, affecting several species of pine trees (*Pinus* spp.) and resulting in huge economic and environmental losses (26–28). PWD was first discovered on Japanese black pine (*Pinus thunbergii* Parl.) in China in 1982 in Purple Mountain Park, Nanjing, China, where the vegetation type is a pure conifer forest established in the late 1970s (29, 30). Since then, the disease has rapidly spread in China and continuously killed conifer trees. Currently, the forest in Nanjing Zijin Mountain Park is still undergoing forest succession from conifer of *P. thunbergii* and *Pinus massoniana* to deciduous trees of *Liquidambar formosana* (Sweetgum) and *Quercus* spp. (Oak) due to the occurrence of PWD. In the current study, we selected three typical forest types representing the entire forest succession process from initial conifer forest to intermediate mixed forest and eventual pure broadleaved forest. The three forests include a pure forest (*P. thunbergii*), a mixed pine and broadleaved forest (*P. thunbergii* + *L. formosana*), and a pure broadleaved forest (*L. formosana*). The intermediate mixed forest is defined by the equal ratio (1:1) between *P. thunbergii* and *L. formosana* trees (31). The eventual pure broadleaved forest is defined by the last pine tree being recently removed due to PWD. As PWD is the only and continuous driving force for forest decline and subsequent succession, our hypothesis is that the response of soil microbes in such a process might differ from those in which the driving forces are transient, such as fire, storm, or lightning. Therefore, the aims of the study are (i) to elucidate the changes in soil enzyme activity and fungal biomass during PWD-induced

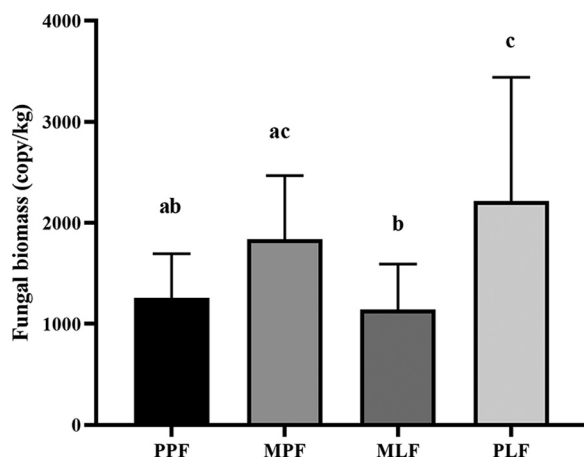


**FIG 1** Soil fungal biomass in pure *P. thunbergii* forest (PPF), mixed forest (MPF + MLF), and pure *Liquidambar* forest (PLF) during forest succession. Letters in the figure show the significant difference ( $P < 0.05$ ) among forest types.

forest succession, (ii) to investigate the response of the soil fungal community structure and function, and (iii) to determine the environmental factors contributing to the dynamic changes in the fungal community during forest succession. To our best knowledge, there is no information available on the dynamic responses of soil microbes to forest succession caused by forest disease.

## RESULTS

**Soil fungal biomass and enzyme activity during forest succession.** The soil fungal biomass differed among forest sites (Fig. 1). The pure *L. formosana* forest (pure *Liquidambar* forest [PLF]) had the highest fungal biomass, which differed from that in the pure pine forest (PPF) and mixed forest (mixed *Liquidambar* forest [MLF]) ( $P < 0.05$ ), whereas the MLF had the lowest fungal biomass. In the mixed forest, the fungal biomass of the mixed pine forest (MPF) was significantly higher than that of MLF ( $P < 0.05$ ).

The soil enzyme activity of  $\beta$ -xylosidase (XYL),  $\beta$ -cellobiosidase (CEL), and  $\beta$ -glucosidase (GLS) involved in the C cycle; phosphatase (PHO) involved in the P cycle; and sulfatase (SUL) involved in the S cycle differed among sites (Table 1). The pure pine forest had the lowest enzyme activities of CEL, GLS, and SUL, which increased during forest succession ( $R^2 = 0.9324$ ,  $R^2 = 0.7895$ , and  $R^2 = 0.6078$ , respectively). The activity of PHO was the highest in the PPF site and differed significantly from that in other sites ( $P < 0.05$ ). The activity of *N*-acetylglucosaminidase (NAG) involved in the N cycle and  $\beta$ -D-glucuronidase (GLR) involved in the C cycle increased ( $R^2 = 0.9466$  and  $R^2 = 0.8883$ , respectively) during the succession.

**Fungal community  $\alpha$ -diversity during forest succession.** In total, 5,664 operational taxonomic units (OTUs) were estimated across all samples. The PPF had the lowest OTU richness ( $349 \pm 99$ ),  $\alpha$ -diversity ( $2.71 \pm 0.65$ ), and evenness ( $0.46 \pm 0.09$ ), among which, the OTU richness significantly differed from that in mixed and PLF sites ( $P < 0.05$ ). The PLF site had significantly higher  $\alpha$ -diversity, richness, and evenness than the PPF site ( $P < 0.05$ ). Interestingly, the diversity index did not differ in the mixed forest between the pine and broadleaved tree species (Fig. 2).

**Fungal community structure at the taxonomic level during forest succession.** All sequences were classified into the fungi domain, including 5 phyla, 12 classes, 20 genera, and 30 species (see Fig. S1 in the supplemental material). Ascomycota was the dominant phylum (42.0%), followed by Basidiomycota (38.0%), Mortierellomycota (9.5%), Mucoromycota (0.2%), and Chytridiomycota (0.1%) (Fig. 3).

The abundances of Ascomycota were the highest in the PLF site, which had the lowest abundance of Basidiomycota (Fig. 3a). Basidiomycota was more abundant in the PPF site. The abundance of Mortierellomycota was also the highest in the PPF site, which differed significantly from that in other sites ( $P < 0.05$ ) (Fig. 3a). *Mortierella* was

**TABLE 1** The soil enzyme activities in the three forests during forest succession<sup>a</sup>

Forest type	C cycle				N cycle NAG	P cycle PHO	S cycle SUL
	XYL	GLR	CEL	GLS			
PPF	16.29 ± 1.74AB	3.12 ± 0.29A	23.91 ± 2.47B	64.52 ± 5.25B	67.73 ± 6.01A	505.89 ± 31.1A	29.04 ± 5.1B
MPF	9.86 ± 1.25B	5.01 ± 1.28A	38.35 ± 5.06B	109.03 ± 15.89B	70.61 ± 7.62A	260.68 ± 24.03B	35.98 ± 7.11B
MLF	16.01 ± 1.72AB	5.77 ± 0.49A	46.97 ± 5.85B	96.36 ± 16.54B	78.21 ± 7.17A	266.55 ± 50.06B	30.22 ± 5.85B
PLF	18.26 ± 2.34A	6.14 ± 0.87A	77.61 ± 9.45A	167.17 ± 17.12A	88.42 ± 10.84A	365.8 ± 33.34B	121.11 ± 22.18A

<sup>a</sup>The data are presented as the mean ± standard deviation. The different letters in the table indicate significant difference ( $P < 0.05$ ) among forest types. PPF, pure *P. thunbergii* forest; MPF, mixed *P. thunbergii* forest; MLF, mixed *L. formosanus* forest; PLF, pure *L. formosanus* forest; XYL,  $\beta$ -xylosidase; GLR,  $\beta$ -D-glucuronidase; CEL,  $\beta$ -cellulobiosidase; GLS,  $\beta$ -glucosidase; NAG, N-acetylglucosaminidase; PHO, phosphatase; SUL, sulfatase.

the most abundant genus at the genus level, followed by *Penicillium*, *Russula*, *Lactarius*, *Clavulina*, *Trichoderma*, *Sebacina*, *Geminibasidium*, *Solicocozyma*, and *Sistotrema* (see Fig. S2 in the supplemental material).

*Mortierella humilis* was the most abundant species at the species level, followed by *Lactarius salmonicolor*, *Russula sanguinea*, and *Mortierella minutissima* (Fig. 3b). Compared to the MPF site, the PPF site had higher abundances of *Mortierella humilis*, *Lactarius salmonicolor*, and *Russula sanguinea* but a lower abundance of *Mortierella exigua*. In the *Liquidambar* forest, the PLF had a higher abundances of *Mortierella minutissima*, *Solicocozyma terricola*, *Amanita fuliginea*, and *Elaphomyces muricatus* than the mixed MLF. The MPF had a higher abundance of *Mortierella exigua* than the MLF site (Fig. 3b).

**Fungal community structure at OTU level during forest succession.** The three forest types shared 13.5% of the total OTUs (765) (Fig. 4). The number of unique OTUs in each forest increased during the succession process; the PPF site had the lowest number of unique OTUs (347, 6.1%), and the PLF site harbored the highest number of unique OTUs (700, 12.4%) (Fig. 4). Distance-based redundancy analysis (dbRDA) based on the OTU data showed that the three forest types formed distinct fungal community structures, and subsequent permutational multivariate analysis of variance (PERMANOVA) confirmed the difference among the communities ( $P < 0.05$  in all pairs) (Fig. 5a). Interestingly, the fungal community structure in the mixed forest between MPF and MLF did not differ. The environmental factors accounted for 15.4% of the total variance and 39.2% of fitted for fungal communities on dbRDA1 as well as for 5.5% of total variation and 13.9% of fitted for fungal communities on dbRDA2. The distance-based linear model (DistLM) using the environmental factors as explanatory variables showed that the tested environmental factors were significantly correlated with fungal communities ( $P < 0.05$  for each of the variables) (Fig. 5a). The soil pH and soil organic carbon (SOC), as well as the ratio of fungal and bacterial biomass (F:B) were positively correlated with the fungal community in the mixed sites (MLF and MPF). The fungal biomass (FB) and the activity of acid phosphatase (PHO) were significantly correlated with the fungal community in the PPF site. The activity of cellobiohydrolase (CEL) was significantly correlated with the fungal community in the PLF site.

**Fungal community structure of predicted function during forest succession.** In total, 2,304 OTUs were included in the FUNguild analysis. The symbiotrophs comprised the

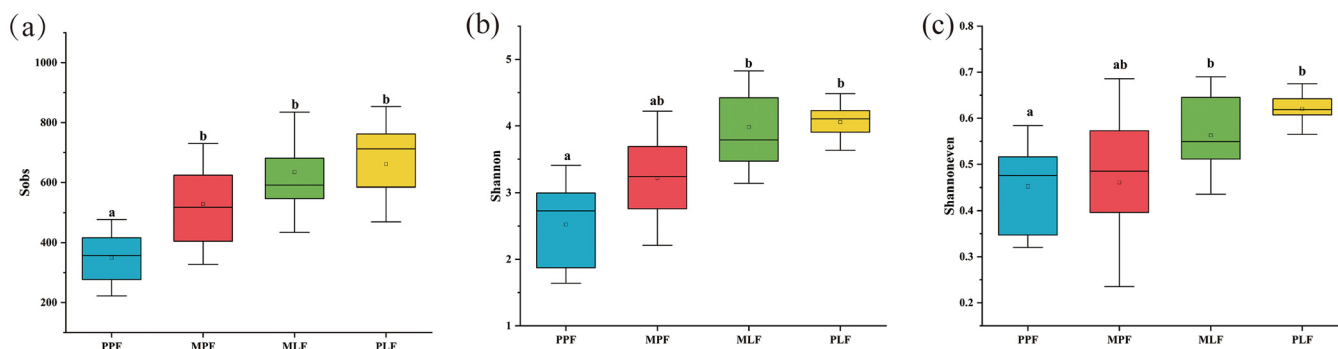


**FIG 2** Fungal community richness (a),  $\alpha$ -diversity (b), and evenness (c) in pure *P. thunbergii* forest (PPF), mixed forest (MPF + MLF), and pure *Liquidambar* forest (PLF) during forest succession. Letters in the figure show the significant difference ( $P < 0.05$ ).

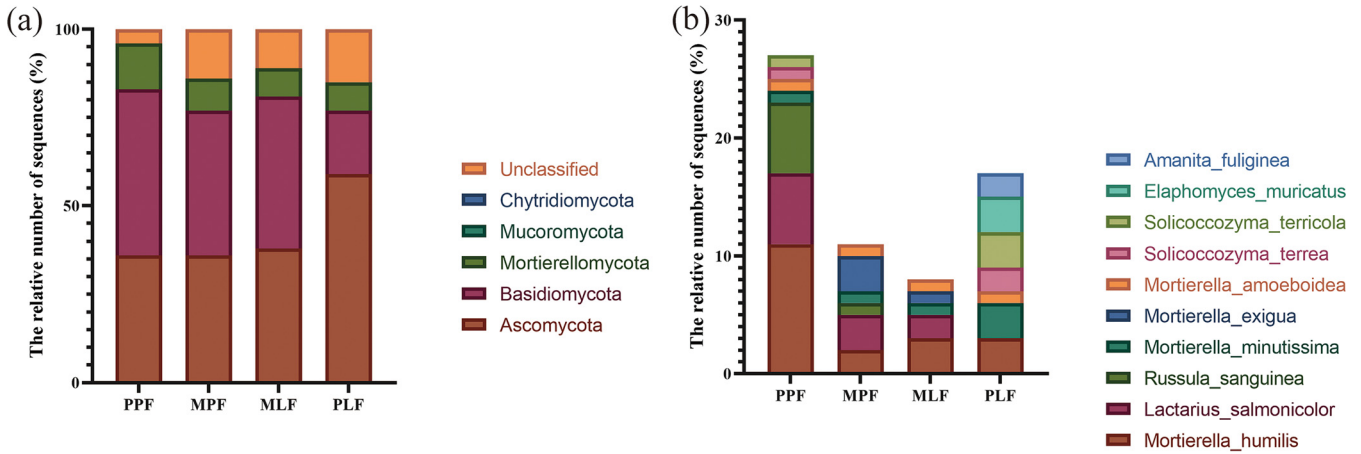


**FIG 3** (a) The most abundant fungal groups at the phylum level. (b) The top 10 species in pure *P. thunbergii* forest (PPF), mixed forest (MPF + MLF), and pure *Liquidambar* forest (PLF) during forest succession.

most dominant trophic mode, covering 31.8% of assigned sequences, followed by the saprotrophs-symbiotrophs (25.5%), saprotrophs (21.4%), pathotrophs-saprotrophs-symbiotrophs (11.5%), pathotrophs (4.9%), pathotrophs-symbiotrophs (2.8%), and pathotrophs-saprotrophs (2.1%) (Fig. 6). During the succession, the abundance of symbiotrophs increased in the mixed forest (MPF and MLF) and decreased significantly in the PLF ( $P < 0.01$ ). The abundance of saprotrophs-symbiotrophs increased in the MPF and then decreased sharply in the mixed and pure *Liquidambar* forest (MLF and PLF). The abundance of saprotrophs differed among the three forest types ( $P < 0.01$ ), in which the PPF had the highest abundance and the mixed forests (MPF and MLF) had the lowest abundance. The pathotrophs had the lowest abundance in the PPF site and increased significantly after the succession ( $R^2 = 0.661$ ). Similarly, the abundances of pathotrophs-symbiotrophs, pathotrophs-saprotrophs, and pathotrophs-saprotrophs-symbiotrophs also increased during forest succession ( $R^2 = 0.704$ ,  $R^2 = 0.785$ ,  $R^2 = 0.995$ , respectively). Some specific functional groups (guilds) significantly differed in abundance among forests during succession (see Fig. S3 and S4 in the supplemental material).

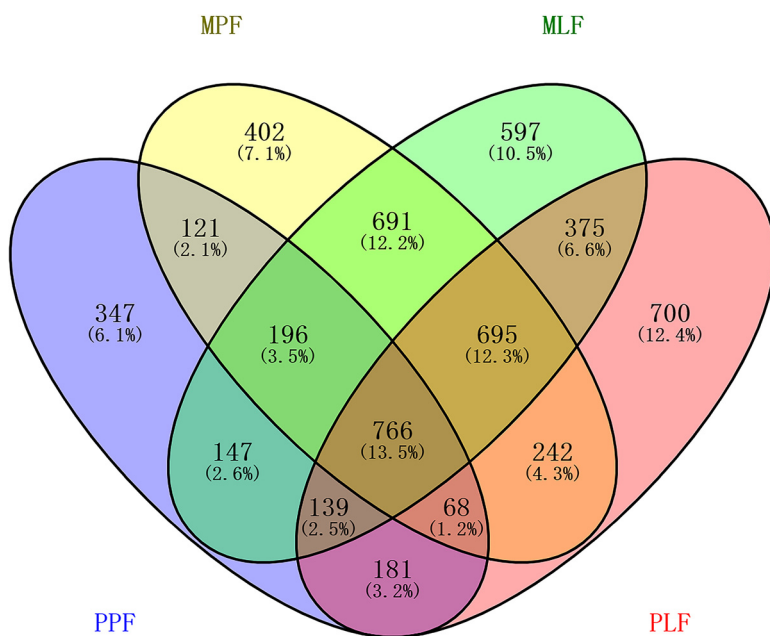


**FIG 4** Venn diagrams showing the unique and shared fungal OTUs among pure *P. thunbergii* forest (PPF), mixed forest (MPF + MLF), and pure *Liquidambar* forest (PLF) during forest succession.

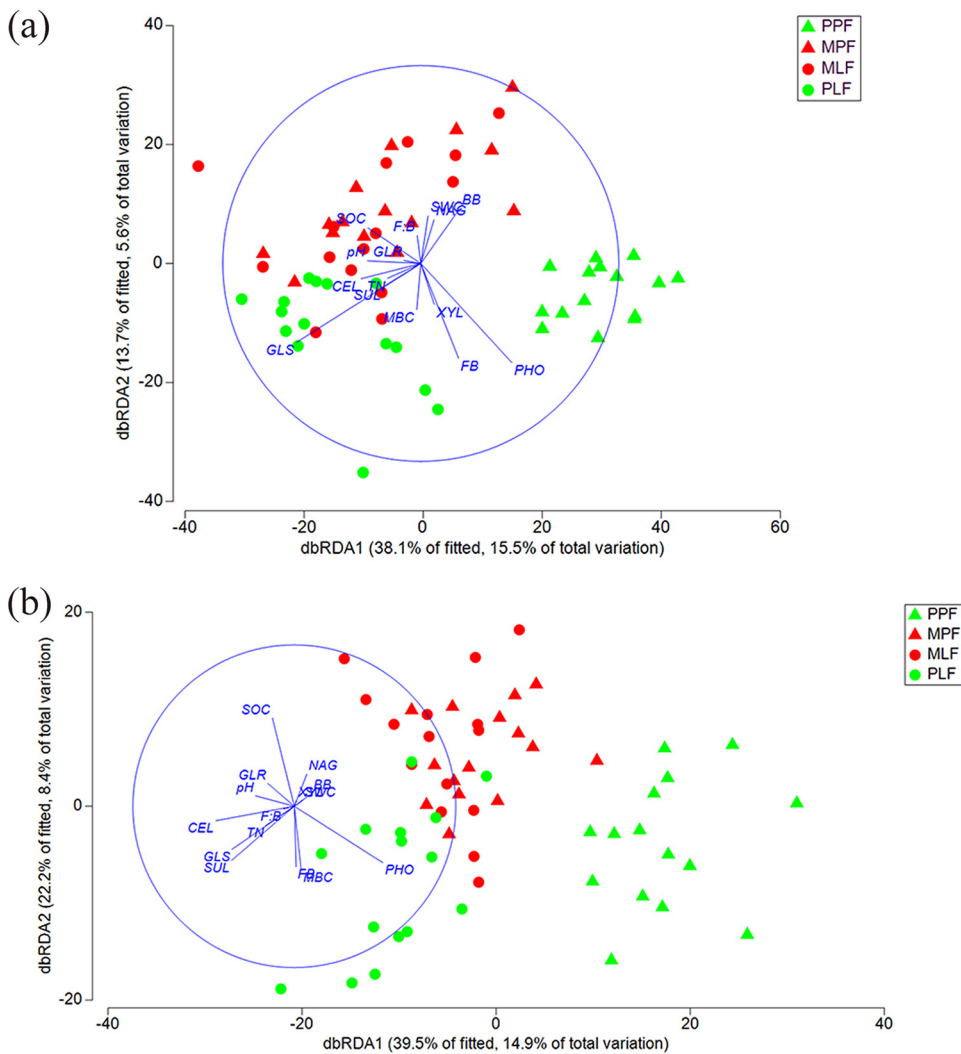


**FIG 5** Distance-based redundancy analysis (dbRDA) showing fungal community structure (a) and functional structure (b) in the three forests among pure *P. thunbergii* forest (PPF), mixed forest (MPF + MLF), and pure *Liquidambar* forest (PLF) using environmental factors as explanatory variables during forest succession.

Distance-based redundancy analysis based on the functional groups showed that the three forest types formed separated functional structures (Fig. 5b). Subsequent PERMANOVA confirmed the differences in functional structures ( $P < 0.05$  in all pairs). However, the functional structures did not differ in a mixed forest between MPF and MLF. The DistLM analysis showed that the soil pH, SOC, total nitrogen (TN), F:B, CEL, GLR, and SUL were significantly correlated with the functional structure in the mixed forest ( $P < 0.05$ ), whereas the enzyme activities of PHO and fungal biomass were significantly corrected with the PPF site ( $P < 0.05$ ). The activities of CEL, GLS, and fungal biomass were significantly correlated with the PLF site ( $P < 0.05$ ) (Fig. 5b).

## DISCUSSION

**Soil fungal biomass, enzyme activity, and fungal  $\alpha$ -diversity during forest succession.** We observed significant differences in fungal biomass among the three forests. The fungal biomass is a determinant of enzyme activities in forest soil (32) and contributes to total microbial biomass (33). Increased fungal biomass could indicate faster litter composition in the soil (34), affecting fungal biomass (35). The fungal biomass in the pure *L. formosana* forest (PLF) was significantly higher than that in the other sites, which is in line with a previous study that suggested that the deciduous

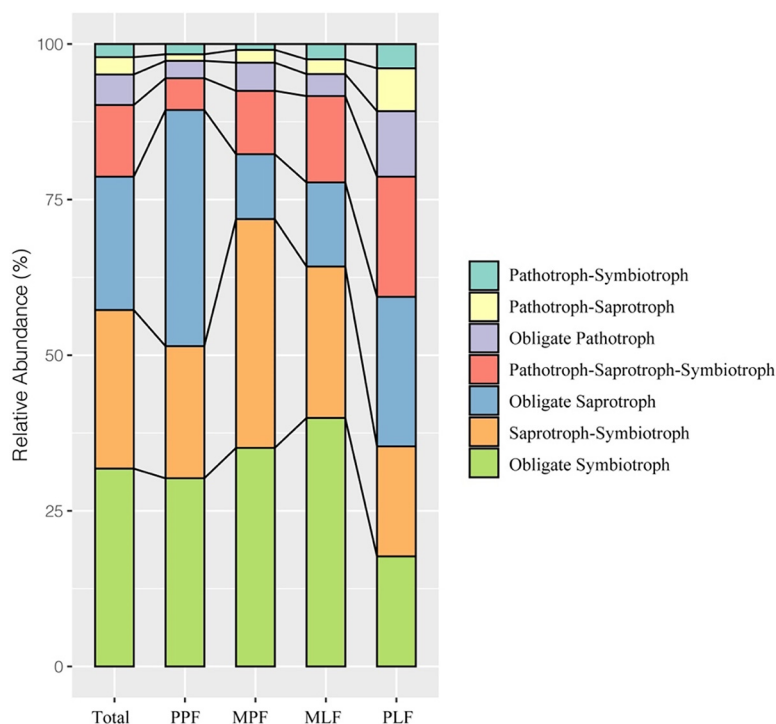


**FIG 6** The fungal functional composition in pure *P. thunbergii* forest (PPF), mixed forest (MPF + MLF), and pure *Liquidambar* forest (PLF) during forest succession.

forest has a significantly higher soil fungal biomass than that of the conifer forest (15). The discrepancies in changes in aboveground plants could partly contribute to this observation. The litter input in pure *L. formosana* forest contains more easily available nutrients for fungi than the pure pine forest. The contents of fungal biomass increased during forest succession, which may indicate the faster decomposition rate due to the shift from conifer to broadleaved trees.

The shift in aboveground plant species caused by forest succession can affect the plant residue biochemistry and the amount and stability of the soil C pool via changing the aggregate allocation of carbon (36, 37). In this study, the enzyme activities in C, N, and S cycles increased during forest succession. The enzyme involved in the C cycle showed higher activities in the PLF forest than those in the other forests, positively correlated with soil fungal biomass. The PPF forest had a lower soil pH with a low soil organic carbon content than that of the other forests, which may explain the lower enzyme activity in the C cycle in the PPF forest. Different tree types can affect the ratio of soil fungi and bacteria by increasing the biomass of fungi over bacteria, which can alter soil enzyme activities (38). This might also explain the difference in enzyme activities among the three forests. In our study, the *N*-acetylglucosaminidase (NAG) and sulfatase activities were significantly higher in the PLF site. NAG is involved in the decomposition of chitin and fungal mycelium (39), and sulfatase is involved in the hydrolyzation of sulfate esters (40). Previous studies have indicated that the activities of both enzymes were correlated positively with soil microbial biomass (38, 41). The NAG and sulfatase activities being significantly higher in the PLF may result from the increased fungal biomass, which can also explain the significantly increased fungal  $\alpha$ -diversity and richness in the PLF site. Moreover, microbes under low P availability might be forced to release phosphatase to meet the demand of P for further growth (42), which causes the higher PHO activity in the initial pure pine forest.

**Soil fungal community structure at OTU and taxonomic levels during forest succession.** The three forests during the succession formed distinct soil fungal communities in our study. The plant species can strongly affect the soil microbial community structure by allocating plant C and other nutrients (8, 9). The variation in tree species in the

three forest types could be the key contributor to the observation. The physiochemical properties of soil (e.g., soil pH and nutrient availability) can be altered by tree species (41), which are important regulators affecting soil microbial communities (10, 11). Soil pH and soil C and N content also significantly differed among the three forests during the succession in our study (see Table S1 in the supplemental material). Interestingly, the fungal community structures in the mixed forest between MPF and MLF did not differ. A similar result was observed for the bacterial community in the same sites in our previous study (31). A previous study has also found that forest type strongly impacts microbial community structure at nutrient-poor sites but less at nutrient-rich sites (43). Therefore, further studies are necessary to elucidate the possible reasons.

Ascomycota, Basidiomycota, and Mortierellomycota were the dominant phyla during forest succession, which is consistent with the results of previous studies where they were the main soil fungal groups (44). During forest succession, the abundance of Ascomycota increased, whereas that of Basidiomycota decreased with the accumulation of soil nutrients. Following forest vegetation restorations, similar results were obtained due to different land uses on the Loess Plateau (45). *Mortierella* and *Penicillium* were the dominant genera during forest succession, reflecting the changes in the availability of nutrients and competition between species. *Penicillium* can degrade cellulose in the early stages of decomposition (46). *Mortierella* spp. can transform phosphorus from an insoluble to a soluble form for plant uptake (47).

The soil properties as explanatory variables were all correlated with the fungal community structures in the study. Previous studies have shown that SOC, soil pH, and TN are factors influencing the fungal community structure (48, 49). Among these, soil pH was one of the essential variables, which showed a positive correlation with Ascomycota fungi (50, 51). However, we did not detect a correlation between the abundance of Ascomycota and soil pH. The range of soil pH in our study was small, which may be attributed to fungi being less sensitive to pH changes than bacteria (52). This could be the reason why it was difficult to ascertain such a correlation.

#### **Fungal community structure of predicted function during forest succession.**

Functionally, the fungal trophic modes (saprotroph, symbiotroph, and pathogen) showed different trends during the succession. The abundance of saprotrophs in the mixed forest (MPF and MLF) was significantly lower than that in the pure forests (PPF and PLF). The abundance of saprophytic fungi can be linked to the plant tree species, most likely due to the difference in the biochemistry of litter input, and the mixed litter may inhibit the degradation process of saprophytic fungi (53). The abundance of symbiotrophs was higher in the mixed forests than that in the pure forests. The mixed forests in our study had higher abundance of ectomycorrhizal (ECM) fungi and SOC content than other forests, which is in line with a previous finding that soil organic matter has a positive correlation with ECM fungi (54, 55). Pathotrophic fungi are suspected of causing diseases or negatively affecting plant performance because they derive nutrient substances by attacking host cells (56). Despite being less abundant during forest succession, the relative abundance of pathotrophs increased during succession. The weakened tree caused by pine wilt disease could increase the occurrence of needle disease and pathogens (57). A previous study indicated that the changes in pathogens could indicate a complex interaction between soil and plants, and increased vegetation, for example, has increased the heterogeneity of the litter, which can provide diverse ecological niches for pathogens (58).

**Conclusion.** The forest succession induced by pine wood nematode disease significantly increased the fungal biomass, soil enzyme activity, and fungal diversity. The forests in different stages of succession formed a distinct fungal community and functional structures in which the fungal community shifted from Basidiomycota dominance in the initial conifer forest to a higher abundance of Ascomycota in the eventual broadleaved forest. Moreover, the symbiotrophs were the most dominant group and the abundance of pathotrophs increased during the succession. Functionally, saprotrophs, symbiotrophs, and pathotrophs dominated the fungal community in the initial forest, mixed forest, and eventual

forest, respectively. The soil pH and SOC were the most important factors affecting the fungal community and functional structure, indicating the importance of environmental factors in shaping microbial community. These findings provide new insight into the responses of microbes to disease-induced forest succession and also highlight the importance of the linkage between plants and microbes in the forest ecosystem.

## MATERIALS AND METHODS

**Study sites and soil sampling.** The study sites are in Nanjing Zijin Mountain Park, Nanjing, Jiangsu Province, China. The mountain area covers approximately 4,500 ha with a latitude of 32°03'22.73" N and longitude of 118°51'26.07" E. The altitudes above sea level at the top and foot of the mountain are approximately 449 and 20 m, respectively. This region belongs to the transitional zone of the subtropical monsoon climate. The annual average precipitation is 1,000 mm, and the average sunshine hours are approximately 2,213 h per year. The annual mean temperature is 15.4°C, ranging from 40.7°C in August to -14.0°C in January (59).

The soil samples were collected in November 2017, and more details were described previously (31). Briefly, three forest types were chosen, including one pure *P. thunbergii* forest (PPF), one pure *L. formosana* forest (PLF), and one mixed forest of *P. thunbergii* and *L. formosana* (MPF and MLF). The ratio of *P. thunbergii* and *L. formosana* trees in mixed forest is about 1:1. The ground vegetations are mainly shrubs in each forest, e.g., *Serissa japonica* (Thunb.) in the PPF site, *Symplocos paniculata* and *Lindera glauca* in mixed forest, and *Smilax china* and *Smilax glaucocchina* in PLF forest. Each forest type had three plots with dimensions of 50 m by 50 m each and were situated 500 m apart from each other. Five trees of *P. thunbergii* or *L. formosana* were randomly chosen in each plot. The soil was collected at a depth of 0 to 10 cm after litter removal in three directions with a 120° angle around each tree and mixed as one sample, resulting in 60 samples in total (15 samples per pure forest + 30 samples in mix forest). The soil samples were placed on ice and delivered to the laboratory for further analysis.

**Soil enzyme activity analysis.** Seven commonly reported soil enzyme activities related to C, N, S, and P cycles were determined. The enzymes involved in the C cycle included  $\beta$ -xylosidase (XYL),  $\beta$ -D-glucuronidase (GLR),  $\beta$ -cellobiosidase (CEL), and  $\beta$ -glucosidase (GLS), and those involved in N, P, and S cycles included *N*-acetylglucosaminidase (NAG), phosphatase (PHO), and sulfatase (SUL), respectively. The soil enzyme activity was measured fluorometrically with a 96-well plate using 4-methylumbelliferone-linked (4-MUB) enzyme substrates following a previously described method (60). Briefly, 2 g of soil sample (fresh weight) was added into a 30-mL acetate buffer solution (50 mM with pH 5) in a 50-mL centrifuge tube. The soil suspensions were shaken at 180 rpm for 40 min at 25°C to break large soil particles followed by the addition of 170 mL sodium acetate solution to 200 mL. The 200  $\mu$ L suspension was added into each well of the 96-well plate followed by the addition of 50  $\mu$ L of 4-MUB-linked substrate (200 mM) to start the reaction. Each soil sample had four replicates. For each replicate, four reactions were also included as follows: blanks (200  $\mu$ L substrate with 50  $\mu$ L double-distilled water), quench standards (200  $\mu$ L substrate with 50  $\mu$ L 4-MUB), negative controls (200  $\mu$ L buffer solution with 50  $\mu$ L 4-MUB-linked substrate), and reference standards (200  $\mu$ L buffer solution with 50  $\mu$ L 4-MUB). Then, 10  $\mu$ L NaOH (1 M) was added to each well to cease the reaction after incubation for 4 h at 25°C in the dark. The fluorescence was measured using a microplate fluorometer with 365-nm excitation and 450-nm emission filters. The enzyme activities were expressed as MUB released in nmol per gram dry soil per hour ( $\text{nmol} \cdot \text{g}^{-1} \cdot \text{h}^{-1}$ ).

**DNA extraction, amplification of ITS rRNA region, Illumina MiSeq, Sequencing, and qPCR for fungal biomass.** The soil genomic DNA was extracted from 0.3 g fresh soil using the Power Soil DNA isolation kit (OMEGA BIO TEK, Norcross, GA, USA) following the manufacturer's instructions. The extracted DNA was measured using a NanoDrop 1000 spectrometer (NanoDrop Technologies, Wilmington, DE, USA) and checked by gel electrophoresis. The DNA product was subjected to the PCR amplification of the internal transcribed spacer 1 (ITS1) region using the primer set ITS1F (5'-CTTGGTCATTAGAG GAAGTAA-3') and ITS2R (5'-GCTGCGTCTTCATCGATGC-3') with a thermocycler PCR system (GeneAmp 9700, ABI, USA). The PCRs were performed in triplicate in a 20- $\mu$ L mixture containing 4  $\mu$ L of 5 $\times$  FastPfu buffer, 2  $\mu$ L of 2.5 mM deoxynucleoside triphosphates (dNTPs), 0.8  $\mu$ L of each primer (5  $\mu$ M), 0.4  $\mu$ L of FastPfu polymerase, 0.2  $\mu$ L of bovine serum albumin (BSA), and 10 ng of template DNA, and the remaining volume was replenished with double-distilled water. The PCRs were conducted using the following program: 3 min of denaturation at 95°C, 36 cycles of 30 s at 95°C, 30 s for annealing at 55°C, 45 s for elongation at 72°C, and a final extension at 72°C for 10 min. The PCR products were checked and extracted from a 2% agarose gel and further purified using the AxyPrep DNA gel extraction kit (Axygen Biosciences, Union City, CA, USA) and quantified using QuantiFluor-ST (Promega, USA) according to the manufacturer's protocol. The purified amplicons were subjected to sequencing with a paired end (PE = 300) on the Illumina MiSeq platform (Illumina, San Diego, USA) according to the standard protocols at Majorbio Bio-Pharm Technology Co. Ltd. (Shanghai, China).

The fungal biomass (FB) in the soil was detected by quantitative PCR (qPCR). The fungal 18S rRNA genes were amplified using the specific-primer pair FF390 (5'-ATTACCGCGTCTGCTGG-3') and FR1 (5'-AIC-CATTCAATCGGTAIT-3') (61). The qPCR was executed using a Bio-Rad CFX96 iCycler on 96-well white-welled polypropylene plates (62). The 20  $\mu$ L reaction mixture contained a 1 $\times$  SsoAdvanced

universal SYBR green supermix (Bio-Rad, USA), 3 ng of template DNA, 250 nM forward primer, and 250 nM reverse primer. The reaction condition was as follows: initial denaturation at 95°C for 3 min, denaturation at 95°C for 15 s, and combined annealing and extension at 60°C for 1 min over 40 cycles. The melting curve analysis was conducted after PCR was run by raising the temperature from 65 to 95°C (0.5°C per 5 s).

The stand curves were conducted using DNA extracted from *Phlebia radiata* FBCC43 (genome size 40.92 Mb; FBCC culture collection, University of Helsinki, Finland). The copy number of the 18S rRNA gene was known (63). The fungal biomass in each sample was calculated based on the standard curve described previously (63).

**Sequence data processing and statistical analysis.** The paired-end sequences were processed using Mothur software (version 1.44.3) following the standard operating procedure (SOP) with some modifications (64, 65). The sequences were screened out if they contained ambiguous (N) bases, homopolymers longer than 8 bp, average quality score lower than 25, putative chimeras (using UCHIME in Mothur), and fewer than 250 bp. The amplification errors were checked using the PCR.seq command. The sequences were pairwise aligned using the align.seq command and preclustered with two base pair differences to remove sequences that were likely due to sequencing errors (66). The high-quality and unique sequences were classified against the UNITE database (version 8) with the bootstrap cutoff as 80 (67). The remove lineage command removed nonfungal sequences. The fungal sequences were then clustered into operational taxonomic units (OTUs) with 97% similarity using the average neighbor-joining algorithm. All global singletons (OTUs containing only one sequence across all samples) were omitted as being of uncertain origin (68). The fungal community species richness (Sobs),  $\alpha$ -diversity (Shannon), and species evenness (Shannoneven) were calculated by subsampling the sequences with the minimum size of the sample among all samples.

The OTUs were assigned into functional groups using the FUNGuild database, in which the fungi were divided into three trophic modes, namely, pathotrophs, symbiotrophs, and saprotrophs (69). Within these trophic modes, fungi were further divided into a total of 21 categories, broadly referred to as guilds. For example, the pathotrophs include plant pathogens, animal pathogens, and fungal parasites. The symbiotrophs include arbuscular mycorrhizal fungi, ectomycorrhizal fungi (ECM), ericoid mycorrhizal fungi (ErM), and endophytes. The saprotrophs include plant saprotrophs, dung saprotrophs, litter saprotrophs, undefined saprotrophs, and wood saprotrophs.

One-way analysis of variance by Duncan's tests was used to determine the significant differences ( $P < 0.05$ ) in fungal  $\alpha$ -diversity, fungal biomass, and enzyme activities among samples in SPSS 21.0 for Windows (SPSS Inc., Chicago, USA). Distance-based redundancy analysis (dbrDA) and permutational multivariate analysis of variance (PERMANOVA) were used to visualize and detect the difference in fungal community and functional structure based on the relative abundance of OTUs or guilds (70). A distance-based linear model (DistLM) was used to test the correlation between the fungal community or functional structure and the environmental variables. The soil properties in the same site from the same project were examined (see Table S1 in the supplemental material). The DistLM analyses were performed in PRIMER 7+ (71). The linear discriminant analysis (LDA) coupled with effect size (LEfSe) (<http://huttenhower.sph.harvard.edu/galaxy>) was used to identify the fungal taxa or FUNGuild differentially represented between samples (72). The LEfSe was performed with an average relative abundance of taxa of  $>0.001$  to hold as many taxa as possible for meaningful comparisons and remove all rare taxa in the analysis. The criteria for the significant difference of fungal taxa and function guilds were set up with  $LDA > 3$  and  $P < 0.05$ . The default value ( $LDA = 2.0$ ) is widely accepted in LEfSe analysis. However, the higher value of LDA can reduce the number of differences in taxa or functional groups and increase the analysis accuracy (73).

**Data availability.** The data sets generated during and/or analyzed during the current study are available in the NCBI Sequence Read Archive (SRA) database (<https://www.ncbi.nlm.nih.gov/sra>) under accession number [PRJNA580298](https://www.ncbi.nlm.nih.gov/sra).

## SUPPLEMENTAL MATERIAL

Supplemental material is available online only.

**SUPPLEMENTAL FILE 1**, PDF file, 0.5 MB.

## ACKNOWLEDGMENTS

The work was supported by the National Natural Science Foundation of China (31870474) and the research funding for Priority Academic Program Development (PAPD) of Jiangsu Higher Education Institutions.

CSC (IT Center for Science Ltd., Finland, <https://www.csc.fi>) is kindly acknowledged for generous computational resources.

We declare that there is no conflict of interest to the submitted work.

A.B. and Z.Q. analyzed and interpreted the data together and wrote the manuscript. A.B., Z.Q., B.L., and Y.M. collected the samples and carried out the lab experiment. H.S. conceived the study, received the research funding, and contributed to the writing. All authors read and approved the final manuscript.

## REFERENCES

- Anderson-Teixeira KJ, Miller AD, Mohan JE, Hudiburg TW, Duval BD, DeLucia EH. 2013. Altered dynamics of forest recovery under a changing climate. *Glob Chang Biol* 19:2001–2021. <https://doi.org/10.1111/gcb.12194>.
- Kardol P, Martijn BT, Van Der Putten WH. 2006. Temporal variation in plant–soil feedback controls succession. *Ecol Lett* 9:1080–1088. <https://doi.org/10.1111/j.1461-0248.2006.00953.x>.
- Sun H, Santalahti M, Pumpanen J, Köster K, Berninger F, Raffaello T, Jumpponen A, Asiegbu FO, Heinonsalo J. 2015. Fungal community shifts in structure and function across a boreal forest fire chronosequence. *Appl Environ Microbiol* 81:7869–7880. <https://doi.org/10.1128/AEM.02063-15>.
- Allison SD, Weintraub MN, Gartner TB, Waldrop MP. 2010. Evolutionary-economic principles as regulators of soil enzyme production and ecosystem function, p 229–243. *In* Soil enzymology. Springer, New York, NY.
- Lasky JR, Uriarte M, Boukili VK, Erickson DL, John Kress W, Chazdon RL. 2014. The relationship between tree biodiversity and biomass dynamics changes with tropical forest succession. *Ecol Lett* 17:1158–1167. <https://doi.org/10.1111/ele.12322>.
- Yan E-R, Wang X-H, Chang SX, He F. 2013. Scaling relationships among twig size, leaf size and leafing intensity in a successional series of subtropical forests. *Tree Physiol* 33:609–617. <https://doi.org/10.1093/treephys/tpt042>.
- Yan E-R, Wang X-H, Huang J-J. 2006. Shifts in plant nutrient use strategies under secondary forest succession. *Plant Soil* 289:187–197. <https://doi.org/10.1007/s11104-006-9128-x>.
- Cotrufo MF, Wallenstein MD, Boot CM, Deneff K, Paul E. 2013. The microbial efficiency-matrix stabilization (MEMS) framework integrates plant litter decomposition with soil organic matter stabilization: do labile plant inputs form stable soil organic matter? *Glob Chang Biol* 19:988–995. <https://doi.org/10.1111/gcb.12113>.
- Khlifa R, Paquette A, Messier C, Reich PB, Munson AD. 2017. Do temperate tree species diversity and identity influence soil microbial community function and composition? *Ecol Evol* 7:7965–7974. <https://doi.org/10.1002/ece3.3313>.
- Bannert A, Kleineidam K, Wissing L, Mueller-Niggemann C, Vogelsang V, Welzl G, Cao Z, Schloter M. 2011. Changes in diversity and functional gene abundances of microbial communities involved in nitrogen fixation, nitrification, and denitrification in a tidal wetland versus paddy soils cultivated for different time periods. *Appl Environ Microbiol* 77:6109–6116. <https://doi.org/10.1128/AEM.01751-10>.
- Prescott CE, Grayston SJ. 2013. Tree species influence on microbial communities in litter and soil: current knowledge and research needs. *Forest Ecol Manage* 309:19–27. <https://doi.org/10.1016/j.foreco.2013.02.034>.
- Bender SF, Plantenga F, Neftel A, Jocher M, Oberholzer H-R, Köhl L, Giles M, Daniell TJ, Van Der Heijden MG. 2014. Symbiotic relationships between soil fungi and plants reduce N<sub>2</sub>O emissions from soil. *ISME J* 8:1336–1345. <https://doi.org/10.1038/ismej.2013.224>.
- Treseder KK, Lennon JT. 2015. Fungal traits that drive ecosystem dynamics on land. *Microbiol Mol Biol Rev* 79:243–262. <https://doi.org/10.1128/MMBR.00001-15>.
- Blagodatskaya E, Kuzyakov Y. 2008. Mechanisms of real and apparent priming effects and their dependence on soil microbial biomass and community structure: critical review. *Biol Fertil Soils* 45:115–131. <https://doi.org/10.1007/s00374-008-0334-y>.
- Noll L, Leonhardt S, Arnstadt T, Hoppe B, Poll C, Matzner E, Hofrichter M, Kellner H. 2016. Fungal biomass and extracellular enzyme activities in coarse woody debris of 13 tree species in the early phase of decomposition. *Forest Ecol Manage* 378:181–192. <https://doi.org/10.1016/j.foreco.2016.07.035>.
- Lin Z, Li Y, Tang C, Luo Y, Fu W, Cai X, Li Y, Yue T, Jiang P, Hu S, Chang SX. 2018. Converting natural evergreen broadleaf forests to intensively managed moso bamboo plantations affects the pool size and stability of soil organic carbon and enzyme activities. *Biol Fertil Soils* 54:467–480. <https://doi.org/10.1007/s00374-018-1275-8>.
- Sinsabaugh RL, Lauber CL, Weintraub MN, Ahmed B, Allison SD, Crenshaw C, Contosta AR, Cusack D, Frey S, Gallo ME, Gartner TB, Hobbie SE, Holland K, Keeler BL, Powers JS, Stursova M, Takacs-Vesbach C, Waldrop MP, Wallenstein MD, Zak DR, Zeglin LH. 2008. Stoichiometry of soil enzyme activity at global scale. *Ecol Lett* 11:1252–1264. <https://doi.org/10.1111/j.1461-0248.2008.01245.x>.
- Baldrian P, Šnajdr J, Merhautová V, Dobiášková P, Cajthaml T, Valášková V. 2013. Responses of the extracellular enzyme activities in hardwood forest to soil temperature and seasonality and the potential effects of climate change. *Soil Biol Biochem* 56:60–68. <https://doi.org/10.1016/j.soilbio.2012.01.020>.
- Sardans J, Peñuelas J, Estiarte M. 2008. Changes in soil enzymes related to C and N cycle and in soil C and N content under prolonged warming and drought in a Mediterranean shrubland. *Appl Soil Ecol* 39:223–235. <https://doi.org/10.1016/j.apsoil.2007.12.011>.
- Cullingham CI, Cooke JE, Dang S, Davis CS, Cooke BJ, Coltman DW. 2011. Mountain pine beetle host-range expansion threatens the boreal forest. *Mol Ecol* 20:2157–2171. <https://doi.org/10.1111/j.1365-294X.2011.05086.x>.
- Cigan PW, Karst J, Cahill JF, Sywenky AN, Pec GJ, Erbilgin N. 2015. Influence of bark beetle outbreaks on nutrient cycling in native pine stands in western Canada. *Plant Soil* 390:29–47. <https://doi.org/10.1007/s11104-014-2378-0>.
- Pec GJ, Karst J, Taylor DL, Cigan PW, Erbilgin N, Cooke JE, Simard SW, Cahill JF, Jr. 2017. Change in soil fungal community structure driven by a decline in ectomycorrhizal fungi following a mountain pine beetle (*Dendroctonus ponderosae*) outbreak. *New Phytol* 213:864–873. <https://doi.org/10.1111/nph.14195>.
- Siqueira JO, Nair MG, Hammerschmidt R, Safir GR, Putnam AR. 1991. Significance of phenolic compounds in plant-soil-microbial systems. *Crit Rev Plant Sci* 10:63–121. <https://doi.org/10.1080/07352689109382307>.
- Hättenschwiler S, Vitousek PM. 2000. The role of polyphenols in terrestrial ecosystem nutrient cycling. *Trends Ecol Evol* 15:238–243. [https://doi.org/10.1016/S0169-5347\(00\)01861-9](https://doi.org/10.1016/S0169-5347(00)01861-9).
- Treu R, Karst J, Randall M, Pec GJ, Cigan PW, Simard SW, Cooke JE, Erbilgin N, Cahill JF. 2014. Decline of ectomycorrhizal fungi following a mountain pine beetle epidemic. *Ecology* 95:1096–1103. <https://doi.org/10.1890/13-1233.1>.
- Alves M, Pereira A, Vicente C, Matos P, Henriques J, Lopes H, Nascimento F, Mota M, Correia A, Henriques I. 2018. The role of bacteria in pine wilt disease: insights from microbiome analysis. *FEMS Microbiol Ecol* 94:fy077. <https://doi.org/10.1093/femsec/fy077>.
- Hirao T, Matsunaga K, Hirakawa H, Shirasawa K, Isoda K, Mishima K, Tamura M, Watanabe A. 2019. Construction of genetic linkage map and identification of a novel major locus for resistance to pine wood nematode in Japanese black pine (*Pinus thunbergii*). *BMC Plant Biol* 19:424. <https://doi.org/10.1186/s12870-019-2045-y>.
- Wang X, Zhu X, Kong X, Mota M. 2011. A rapid detection of the pinewood nematode, *Bursaphelenchus xylophilus* in stored *Monochamus alternatus* by rDNA amplification. *J Appl Entomol* 135:156–159. <https://doi.org/10.1111/j.1439-0418.2010.01529.x>.
- Mota MM, Futai K, Vieira P. 2009. Pine wilt disease and the pinewood nematode, *Bursaphelenchus xylophilus*, p 253–274. *In* Integrated management of fruit crops nematodes. Springer, New York, NY.
- Gao R, Wang Z, Wang H, Hao Y, Shi J. 2019. Relationship between pine wilt disease outbreaks and climatic variables in the three gorges reservoir region. *Forests* 10:816. <https://doi.org/10.3390/f10090816>.
- Qu ZL, Liu B, Ma Y, Xu J, Sun H. 2020. The response of the soil bacterial community and function to forest succession caused by forest disease. *Funct Ecol* 34:2548–2559. <https://doi.org/10.1111/1365-2435.13665>.
- Grierson PF, Adams M. 2000. Plant species affect acid phosphatase, ergosterol and microbial P in a Jarrah (*Eucalyptus marginata* Donn ex Sm.) forest in south-western Australia. *Soil Biol Biochem* 32:1817–1827. [https://doi.org/10.1016/S0038-0717\(00\)00155-3](https://doi.org/10.1016/S0038-0717(00)00155-3).
- Chang E-H, Tian G, Chiu C-Y. 2017. The effect of re-planting trees on soil microbial communities in a wildfire-induced subalpine grassland. *Forests* 8:385. <https://doi.org/10.3390/f8100385>.
- Baldrian P. 2008. Wood-inhabiting ligninolytic basidiomycetes in soils: ecology and constraints for applicability in bioremediation. *Fungal Ecology* 1:4–12. <https://doi.org/10.1016/j.funeco.2008.02.001>.
- Papa S, Cembrola E, Pellegrino A, Fuggi A, Fioretto A. 2014. Microbial enzyme activities, fungal biomass and quality of the litter and upper soil layer in a beech forest of south Italy. *Eur J Soil Sci* 65:274–285. <https://doi.org/10.1111/ejss.12112>.
- Feng Y, Han S, Chen W, Gu Y, Stewart CE, Zhang J, Geng S, Chen Z, Setälä H. 2020. Variation in soil lignin protection mechanisms in five successional gradients of mixed broadleaf–pine forests. *Soil Sci Soc Am J* 84:232–250. <https://doi.org/10.1002/saj2.20032>.
- Tamura M, Suseela V, Simpson M, Powell B, Tharayil N. 2017. Plant litter chemistry alters the content and composition of organic carbon associated with soil mineral and aggregate fractions in invaded ecosystems. *Glob Chang Biol* 23:4002–4018. <https://doi.org/10.1111/gcb.13751>.
- Chung H, Zak DR, Reich PB, Ellsworth DS. 2007. Plant species richness, elevated CO<sub>2</sub>, and atmospheric nitrogen deposition alter soil microbial community composition and function. *Global Change Biol* 13:980–989. <https://doi.org/10.1111/j.1365-2486.2007.01313.x>.

39. Zhou X, Wang SS, Chen C. 2017. Modeling the effects of tree species and incubation temperature on soil's extracellular enzyme activity in 78-year-old tree plantations. *Biogeosciences* 14:5393–5402. <https://doi.org/10.5194/bg-14-5393-2017>.
40. McGill W, Cole C. 1981. Comparative aspects of cycling of organic C, N, S and P through soil organic matter. *Geoderma* 26:267–286. [https://doi.org/10.1016/0016-7061\(81\)90024-0](https://doi.org/10.1016/0016-7061(81)90024-0).
41. Xu J, Liu B, Qu Z-I, Ma Y, Sun H. 2020. Age and species of Eucalyptus plantations affect soil microbial biomass and enzymatic activities. *Microorganisms* 8:811. <https://doi.org/10.3390/microorganisms8060811>.
42. Heitkötter J, Heinze S, Marschner B. 2017. Relevance of substrate quality and nutrients for microbial C-turnover in top- and subsoil of a Dystric Cambisol. *Geoderma* 302:89–99. <https://doi.org/10.1016/j.geoderma.2017.04.029>.
43. Lu J-Z, Scheu S. 2021. Response of soil microbial communities to mixed beech-conifer forests varies with site conditions. *Soil Biol Biochem* 155: 108155. <https://doi.org/10.1016/j.soilbio.2021.108155>.
44. Wu D, Zhang M, Peng M, Sui X, Li W, Sun G. 2019. Variations in soil functional fungal community structure associated with pure and mixed plantations in typical temperate forests of China. *Front Microbiol* 10:1636. <https://doi.org/10.3389/fmicb.2019.01636>.
45. Yang Y, Dou Y, Huang Y, An S. 2017. Links between soil fungal diversity and plant and soil properties on the Loess Plateau. *Front Microbiol* 8: 2198. <https://doi.org/10.3389/fmicb.2017.02198>.
46. Chinedu SN, Okochi V, Omidi O. 2011. Cellulase production by wild strains of *Aspergillus niger*, *Penicillium chrysogenum* and *Trichoderma harzianum* grown on waste cellulosic materials. *Ife J Sci* 13:57–62.
47. Osorio NW, Habte M. 2013. Synergistic effect of a phosphate-solubilizing fungus and an arbuscular mycorrhizal fungus on leucaena seedlings in an Oxisol fertilized with rock phosphate. *Botany* 91:274–281. <https://doi.org/10.1139/cjb-2012-0226>.
48. Ding J, Jiang X, Guan D, Zhao B, Ma M, Zhou B, Cao F, Yang X, Li L, Li J. 2017. Influence of inorganic fertilizer and organic manure application on fungal communities in a long-term field experiment of Chinese Mollisols. *Appl Soil Ecol* 111:114–122. <https://doi.org/10.1016/j.apsoil.2016.12.003>.
49. Liu J, Sui Y, Yu Z, Shi Y, Chu H, Jin J, Liu X, Wang G. 2015. Soil carbon content drives the biogeographical distribution of fungal communities in the black soil zone of northeast China. *Soil Biol Biochem* 83:29–39. <https://doi.org/10.1016/j.soilbio.2015.01.009>.
50. Lauber CL, Strickland MS, Bradford MA, Fierer N. 2008. The influence of soil properties on the structure of bacterial and fungal communities across land-use types. *Soil Biol Biochem* 40:2407–2415. <https://doi.org/10.1016/j.soilbio.2008.05.021>.
51. Yao F, Yang S, Wang Z, Wang X, Ye J, Wang X, DeBruyn JM, Feng X, Jiang Y, Li H. 2017. Microbial taxa distribution is associated with ecological trophic cascades along an elevation gradient. *Front Microbiol* 8:2071. <https://doi.org/10.3389/fmicb.2017.02071>.
52. Ren C, Zhang W, Zhong Z, Han X, Yang G, Feng Y, Ren G. 2018. Differential responses of soil microbial biomass, diversity, and compositions to altitudinal gradients depend on plant and soil characteristics. *Sci Total Environ* 610–611:750–758. <https://doi.org/10.1016/j.scitotenv.2017.08.110>.
53. Francioli D, van Rijssel SQ, van Ruijven J, Termorshuizen AJ, Cotton T, Dumbrell AJ, Raaijmakers JM, Weigelt A, Mommer L. 2021. Plant functional group drives the community structure of saprophytic fungi in a grassland biodiversity experiment. *Plant Soil* 461:91–105. <https://doi.org/10.1007/s11104-020-04454-y>.
54. Zhang Y, Cao H, Zhao P, Wei X, Ding G, Gao G, Shi M. 2021. Vegetation restoration alters fungal community composition and functional groups in a desert ecosystem. *Front Environ Sci* 9:589068. <https://doi.org/10.3389/fenvs.2021.589068>.
55. Suz L, Kallow S, Reed K, Bidartondo M, Barsoum N. 2017. Pine mycorrhizal communities in pure and mixed pine-oak forests: abiotic environment trumps neighboring oak host effects. *Forest Ecol Manage* 406:370–380. <https://doi.org/10.1016/j.foreco.2017.09.030>.
56. Anthony M, Frey S, Stinson K. 2017. Fungal community homogenization, shift in dominant trophic guild, and appearance of novel taxa with biotic invasion. *Ecosphere* 8:e01951. <https://doi.org/10.1002/ecs2.1951>.
57. Liu Y, Qu Z-L, Liu B, Ma Y, Xu J, Shen W-X, Sun H. 2021. The impact of pine wood nematode infection on the host fungal community. *Microorganisms* 9:896. <https://doi.org/10.3390/microorganisms9050896>.
58. Shi L, Dossa GG, Paudel E, Zang H, Xu J, Harrison RD. 2019. Changes in fungal communities across a forest disturbance gradient. *Appl Environ Microbiol* 85:e00080-19. <https://doi.org/10.1128/AEM.00080-19>.
59. Deng S, Katoh M, Guan Q, Yin N, Li M. 2014. Estimating forest above-ground biomass by combining ALOS PALSAR and WorldView-2 data: a case study at Purple Mountain National Park, Nanjing, China. *Remote Sensing* 6:7878–7910. <https://doi.org/10.3390/rs6097878>.
60. Sinsabaugh R, Saiya-Cork K, Long T, Osgood M, Neher D, Zak D, Norby R. 2003. Soil microbial activity in a Liquidambar plantation unresponsive to CO<sub>2</sub>-driven increases in primary production. *Appl Soil Ecol* 24:263–271. [https://doi.org/10.1016/S0929-1393\(03\)00002-7](https://doi.org/10.1016/S0929-1393(03)00002-7).
61. Vainio EJ, Hantula J. 2000. Direct analysis of wood-inhabiting fungi using denaturing gradient gel electrophoresis of amplified ribosomal DNA. *Mycological Res* 104:927–936. <https://doi.org/10.1017/S0953756200002471>.
62. Helin A, Sietiö O-M, Heinonsalo J, Bäck J, Riekkola M-L, Parshintsev J. 2017. Characterization of free amino acids, bacteria and fungi in size-segregated atmospheric aerosols in boreal forest: seasonal patterns, abundances and size distributions. *Atmos Chem Phys* 17:13089–13101. <https://doi.org/10.5194/acp-17-13089-2017>.
63. Zhou X, Sun H, Pumpanen J, Sietiö O-M, Heinonsalo J, Köster K, Berninger F. 2019. The impact of wildfire on microbial C:N:P stoichiometry and the fungal-to-bacterial ratio in permafrost soil. *Biogeochemistry* 142:1–17. <https://doi.org/10.1007/s10533-018-0510-6>.
64. Schloss PD, Westcott SL, Ryabin T, Hall JR, Hartmann M, Hollister EB, Lesniewski RA, Oakley BB, Parks DH, Robinson CJ, Sahl JW, Stres B, Thallinger GG, Van Horn DJ, Weber CF. 2009. Introducing mothur: open-source, platform-independent, community-supported software for describing and comparing microbial communities. *Appl Environ Microbiol* 75:7537–7541. <https://doi.org/10.1128/AEM.01541-09>.
65. Sun H, Terhonen E, Kovalchuk A, Tuovila H, Chen H, Oghenekaro AO, Heinonsalo J, Kohler A, Kasanen R, Vasander H, Asiegbu FO. 2016. Dominant tree species and soil type affect the fungal community structure in a boreal peatland forest. *Appl Environ Microbiol* 82:2632–2643. <https://doi.org/10.1128/AEM.03858-15>.
66. Santalahti M, Sun H, Jumpponen A, Pennanen T, Heinonsalo J. 2016. Vertical and seasonal dynamics of fungal communities in boreal Scots pine forest soil. *FEMS Microbiol Ecol* 92:fiw170. <https://doi.org/10.1093/femsec/fiw170>.
67. Abarenkov K, Henrik Nilsson R, Larsson K-H, Alexander IJ, Eberhardt U, Erland S, Høiland K, Kjoller R, Larsson E, Pennanen T, Sen R, Taylor AFS, Tedersoo L, Ursing BM, Vrålstad T, Liimatainen K, Peintner U, Kõljalg U. 2010. The UNITE database for molecular identification of fungi—recent updates and future perspectives. *New Phytol* 186:281–285. <https://doi.org/10.1111/j.1469-8137.2009.03160.x>.
68. Tedersoo L, Nilsson RH, Abarenkov K, Jairus T, Sadam A, Saar I, Bahram M, Bechem E, Chuyong G, Kõljalg U. 2010. 454 Pyrosequencing and Sanger sequencing of tropical mycorrhizal fungi provide similar results but reveal substantial methodological biases. *New Phytol* 188:291–301. <https://doi.org/10.1111/j.1469-8137.2010.03373.x>.
69. Tedersoo L, Bahram M, Pölme S, Kõljalg U, Yorou NS, Wijesundera R, Villarreal Ruiz L, Vasco-Palacios AM, Thu PQ, Suija A, Smith ME, Sharp C, Saluveer E, Saitta A, Rosas M, Riit T, Ratkowsky D, Pritsch K, Pöldmaa K, Piepenbring M, Phosri C, Peterson M, Parts K, Pärtel K, Otting E, Nounra E, Njouonkou AL, Nilsson RH, Morgado LN, Mayor J, May TW, Majauskim L, Lodge DJ, Lee SS, Larsson K-H, Kohout P, Hosaka K, Hiiesalu I, Henkel TW, Harend H, Guo L-D, Greslebin A, Grelet G, Geml J, Gates G, Dunstan W, Dunk C, Drenkhan R, Dearnaley J, De Kesel A, et al. 2014. Global diversity and geography of soil fungi. *Science* 346:1256688. <https://doi.org/10.1126/science.1256688>.
70. Anderson MJ. 2001. A new method for non-parametric multivariate analysis of variance. *Austral Ecol* 26:32–46. <https://doi.org/10.1111/j.1442-9993.2001.01070.ppx>.
71. Gorley A, Clarke K. 2008. PERMANOVA+ for PRIMER: guide to software and statistical methods. PRIMER-E, Plymouth, UK.
72. Segata N, Izard J, Waldron L, Gevers D, Miropolsky L, Garrett WS, Huttenhower C. 2011. Metagenomic biomarker discovery and explanation. *Genome Biol* 12: R60. <https://doi.org/10.1186/gb-2011-12-6-r60>.
73. Fisher RA. 1936. The use of multiple measurements in taxonomic problems. *Ann Eugenics* 7:179–188. <https://doi.org/10.1111/j.1469-1809.1936.tb02137.x>.